Dielectric properties and electrical percolation in $MnFe_2O_4$/epoxy resin composites

Darya Meisak,[1,2] Jan Macutkevic,[1] Algirdas Selskis[3], Juras Banys,[1] and Polina Kuzhir[4,2]

[1] Physics Faculty, Vilnius University, Vilnius 00122, Lithuania.
[2] Research Institute for Nuclear Problems, Belarusian State University, Minsk 220030, Belarus.
[3] Center for Physical Sciences and Technology, Vilnius 10257, Lithuania.
[4] Institute of Photonics, University of Eastern Finland, Yliopistokatu 7, FI-80101 Joensuu, Finland.

Keywords: dielectric properties, electrical percolation, $MnFe_2O_4$

Broadband dielectric properties of epoxy composites containing the different additions of manganese ferrite ($MnFe_2O_4$) with two spherical particle size (28 and 60 nm) have been studied in the wide temperature range from 150 K to 500 K. The percolation thresholds in such systems are 30 and 29.3 vol.% for small and large $MnFe_2O_4$ particles, respectively. The small difference in the percolation threshold value is related to a better distribution of larger nanoparticles. Composites above the percolation threshold are appropriate candidates for electromagnetic shielding applications. Above 380 K the electrical conductivity is typical for all composites, both below and above the percolation threshold due to the electrical transport in the polymer matrix. The activation energy strongly decreases with $MnFe_2O_4$ concentration indicating that the electrical transport occurs simultaneously in both $MnFe_2O_4$ and epoxy matrix subsystems.

1. Introduction

A composite material, as a heterogeneous system consisting of a polymer matrix and fillers embedded, acquire properties from all its components, which attracts the attention of many researchers. The possibility to control these properties (by a selection of polymer matrix, fillers and fabrication process) makes composites interesting for many applications [1-2].
An excellent candidate for the role of composite inclusions is manganese ferrite ($MnFe_2O_4$), which is considered as one of the most important inorganic materials due to their electrical, optical, magnetic and catalytic properties [3]. Manganese ferrite is characterized by a variety of sizes [4-5] and forms [6-7] and it can also be incorporated in carbon structures [8-9], which also affects their properties. From the magnetic properties point of view, this type of particles is already quite well studied and it is found that magnetic properties of these particles are strongly size-dependent [7]. On this basis, magnetic ferrite particles have found applications in many directions, such as magnetic recording media devices [10], ferrofluid [11], biosensors [12], as well as for biomedical applications (magnetic resonance imaging, magnetic hyperthermia for cancer therapy, cells and DNA separation, etc.) [9].
However, investigations of $MnFe_2O_4$ in terms of electrical properties can be also interesting, in order to make them applicable (along with very popular carbon materials) in fields such as electromagnetic shielding and radar absorbing coatings [13], for electromagnetic compatibility [14]. Nevertheless, the electrical percolation phenomena was not studied in composites with $MnFe_2O_4$ inclusions. Some preliminary estimations of electrical percolation threshold in composites with $MnFe_2O_4$ inclusions were performed in [15], however in the work [15] composites with only several $MnFe_2O_4$ concentations were investigated. The electrical percolation threshold is very important parameter for various practical applications of composites, including electromagnetic shielding [16]. Moreover, the electrical percolation

threshold can be substantially lower than it is expected by theoretical calculations and dependent from particle size, even for round particles [17].
The purpose of this work is to study the dielectric properties of epoxy resin composites filled with manganese ferrite ($MnFe_2O_4$) nanopowder, which has two different spherical particle size (28 and 60 nm).

2. Materials and Methods

The commercially available manganese ferrite ($MnFe_2O_4$) nanopowder with two spherical particle sizes (28 nm and 60 nm) was used as a filler [18-19]. Both nanopowder sizes are easily dispersed in the polymer matrix and enable the production of composites with high volume concentrations.
In this work, a series of composite samples were produced using epoxy resin Epikote 828, a curing agent called triethylenetetramine (TETA) and 10, 20, 23, 25, 28 and 30 vol. % of $MnFe_2O_4$ nanopowder filler. The procedure of composite manufacturing is described in detail in [20]. In summary, the $MnFe_2O_4$ nanopowders were mechanically crushed and stirred in ethanol during half an hour. Then the particles were dispersed in ethanol with an ultrasonic bath for 1 hour. Afterward, the alcoholic suspension of $MnFe_2O_4$ nanopowder was mixed with the epoxy resin and underwent ultrasonication by a probe for 2 hours. After the ethanol evaporation, TETA hardener was added to the resulting mixture of epoxy resin and manganese ferrite particles and mechanically mixed for 5-7 minutes. The blend was poured into molds and left in them for 20 h for the curing process at room temperature, and then for 2 hours in an oven at a temperature of 200°C. All composite preparation technology conditions were varied in order to obtain the lowest percolation threshold; it was determined that the above listed conditions are optimal.
The surface morphology was studied by scanning electron microscopy (SEM) using a Helios NanoLab 650 microscope.
The complex dielectric permittivity was measured using an LCR HP4284A meter in the frequency range from 20 Hz to 1 MHz. Each measurement was followed by heating to 500 K and then cooling to 150 K with rate 1 K/min in an air atmosphere. Silver paste was used for contacting. The measurement's accuracy was better as 1%. The electrical conductivity σ was calculated according to $\sigma = 2\pi\nu\varepsilon_0\varepsilon''$, where ε_0 is the permittivity of vacuum, ε'' is the imaginary part of dielectric permittivity and ν is the measurement frequency.

3. Results and Discussion

3.1 Room-temperature region

SEM images of composites with different size $MnFe_2O_4$ nanoparticles are presented in Fig. 1. It can be concluded that nanoparticles are good distributed in both cases.

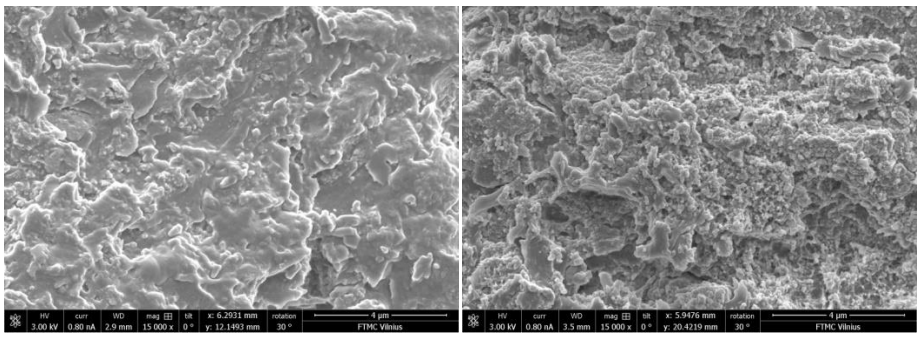

Figure 1. SEM images of composites with different size $MnFe_2O_4$ nanoparticles (left particle size 60 nm, right particle size 28 nm).

The frequency dependence at room temperature of the real part of dielectric permittivity (ε') and the electrical conductivity (σ) of epoxy composites with different $MnFe_2O_4$ (60 nm particle size) loadings is shown in Fig. 2. An increase of the manganese ferrite concentration in epoxy resin leads to the monotonic increase of the dielectric permittivity and electrical conductivity values. Moreover, for composites with a concentration ≤ 20 vol. %, the dielectric permittivity is a completely frequency-independent function, and the DC conductivity plateau is absent (similarly to epoxy resin). However, for composites with concentration > 20 vol. %, the dielectric permittivity is frequency dependent and at a maximum concentration of 30 vol. % ε' decreases strongly with increasing frequency, and a weakly pronounced plateau of σ appears, indicating that the percolation threshold is close to 30 vol. %.

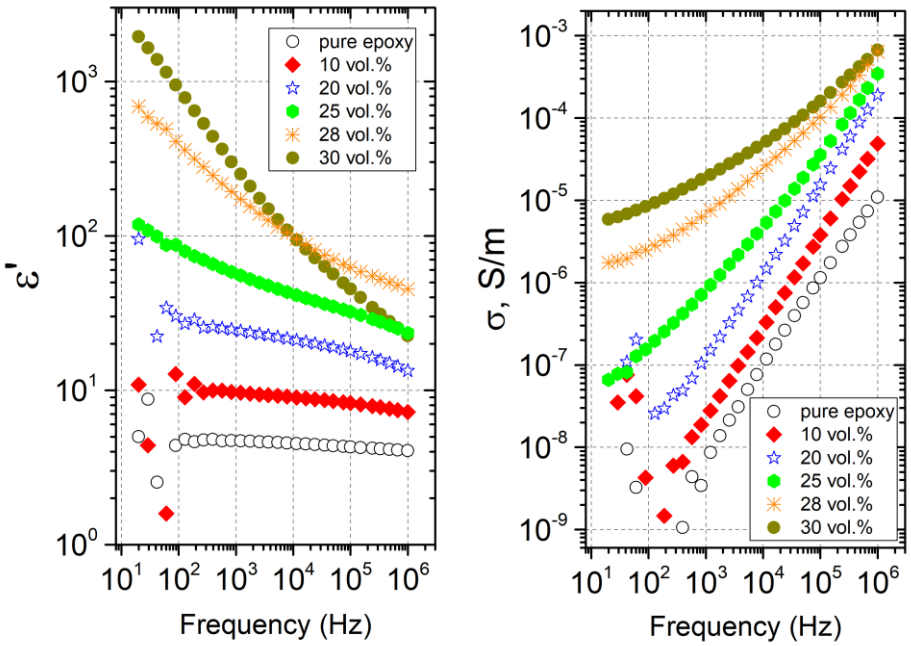

Figure 2. Frequency dependence of the dielectric permittivity (left) and the electrical conductivity (right) for $MnFe_2O_4$/epoxy composites with 60 nm particle size at room temperature.

In order to determine the percolation threshold of composites with 28 nm and 60 nm $MnFe_2O_4$ particle sizes, the dielectric permittivity at 396 Hz and room temperature was plotted as a function of concentration in Fig. 3. Since all the studied concentrations (except the maximum one of 30%) did not have a frequency-independent plateau at low frequencies, the dielectric permittivity was fitted according to the classical power law for composites below the percolation threshold [21]:

$$\varepsilon' = \varepsilon_m (p_c - p)^{-t} \quad (1)$$

where ε_m is the constant, p is the filler concentration, p_c is the critical volume fraction (percolation threshold), and t is the critical exponent. The obtained parameters and their standard errors for composites are presented in Table 1.

Table 1. Parameters of the percolation threshold law fit

	ε_m		p_c, vol.%		t	
	Value	Standard Error	Value	Standard Error	Value	Standard Error
28 nm	91.9	8.8	30	0.691	0.58	0.08
60 nm	330.98	14.56	29.3	0.06	1.13	0.02

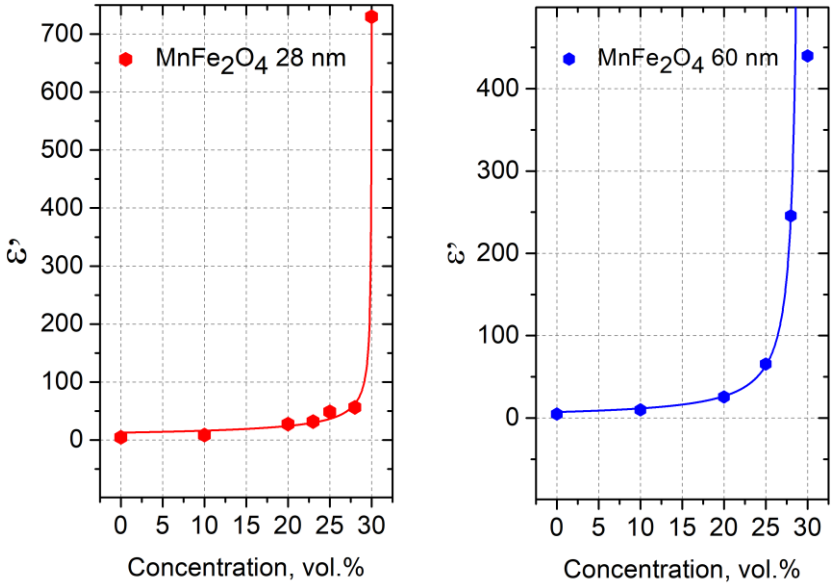

Figure 3. Concentration dependence of the real part of dielectric permittivity for $MnFe_2O_4$/epoxy composites with 28 nm particle size (left) and 60 nm particle size (right) at room temperature and 396 Hz (symbols), and fits with Eq. (1) (solid curves).

This calculation indicates that the electrical percolation for $MnFe_2O_4$/epoxy composites is reached when the filler concentration is close to 30 vol. %. Moreover, it seems that the percolation threshold depends on the size of the manganese ferrite spherical particles. However, according to the excluded volume theory [22], the percolation threshold depends only on the shape of the particles, and not on their size. Therefore, it should be assumed that the difference in the conductive capacity of composites based on different size manganese ferrite is due to their different distribution in the polymer matrix.

3.2 Temperature-dependent region

Let's consider the typical behavior of a composite below the percolation threshold using a sample with 20 vol. % $MnFe_2O_4$ (60 nm particle size) as an example. For this composite temperature dependences of the complex dielectric permittivity at different frequencies and frequency dependences of complex dielectric permittivity at different temperatures are shown in Figures 4, 5 respectively. For comparison in Fig. 4 the data for pure epoxy resin is plotted. In the temperature range 150–250 K, the imaginary part of ε versus T and ν is characterized by maxima, whose position is frequency- and temperature-dependent, respectively. With increasing frequency, the maximum of $\varepsilon''(T)$ expands and shifts towards higher temperatures (see Fig. 4, right), while during cooling the maximum of $\varepsilon''(\nu)$ expands and shifts towards lower frequencies (see Fig. 5, right). The real part of ε versus T (see Fig. 4, left) and ν (see Fig. 5, left) decreases with increasing frequency and decreasing temperature respectively. Similar behavior was observed for each composite below the percolation threshold of both sizes, as well as for pure epoxy (see open symbols in Fig. 4). This behavior is due to the dipole relaxation [23].

The relaxation time, defined as the reciprocal frequency value at the maximum of the imaginary part at a fixed temperature, increases according to the Vogel-Fulcher law with cooling (see Figure 6):

$$\tau = \frac{1}{\nu_{max}} = \tau_0 e^{\frac{E_B}{k_B(T-T_0)}} \quad (2)$$

where τ_0 is the relaxation time at very high temperatures, E_B is the activation energy, and T_0 is the glass transition temperature.
The approximation parameters and their standard errors are presented in Table 2.

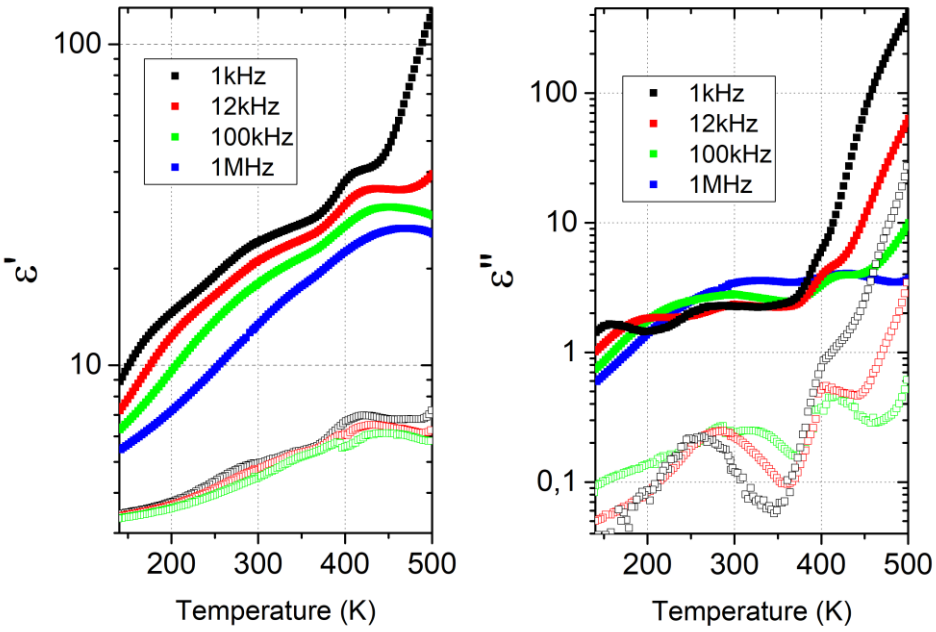

Figure 4. Temperature dependence of the complex dielectric permittivity for pure epoxy resin (open symbols) and epoxy composite (close symbols) with 20 vol. % $MnFe_2O_4$ (60 nm particle size) at different frequencies.

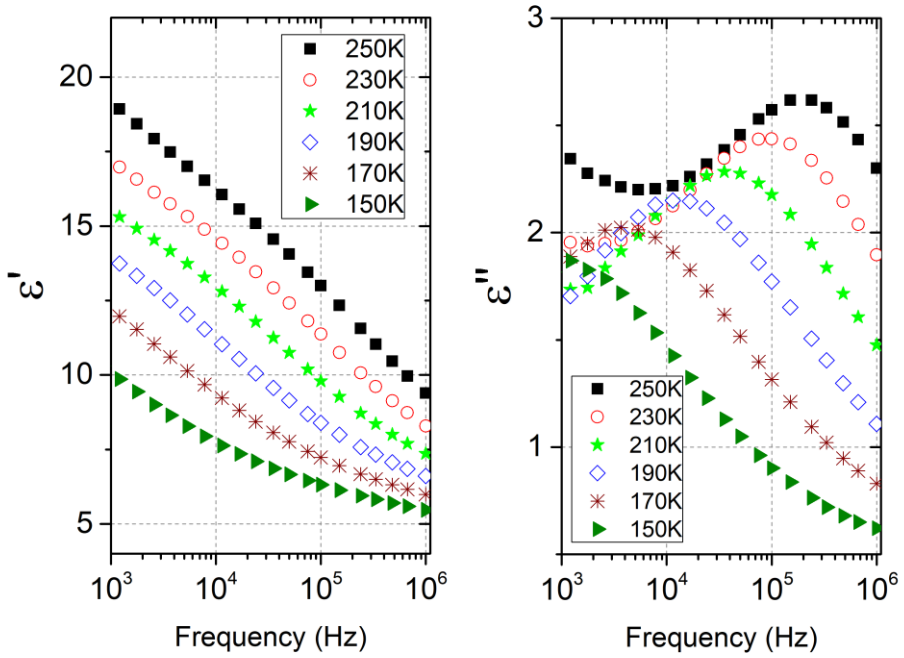

Figure 5. Frequency dependence of complex dielectric permittivity for epoxy composite with 20 vol. % $MnFe_2O_4$ (60nm particle size) at different temperatures.

Table 2. Parameters of the Vogel-Fulcher law fit of the relaxation time

Concentration, vol.%	Particle size, nm	$\ln\{\tau_0, s\}$		E_B/k_B, K		T_0, K	
		Value	Standard Error	Value	Standard Error	Value	Standard Error
Pure resin	-	-23	0	1969	91	137	7.7
10	28	-15	0	634	124	74	22
20	28	-16.5	0	798	39	80	5.7
10	60	-16.5	0	672	78	83	12
20	60	-16.5	0	782	34	77	5.1

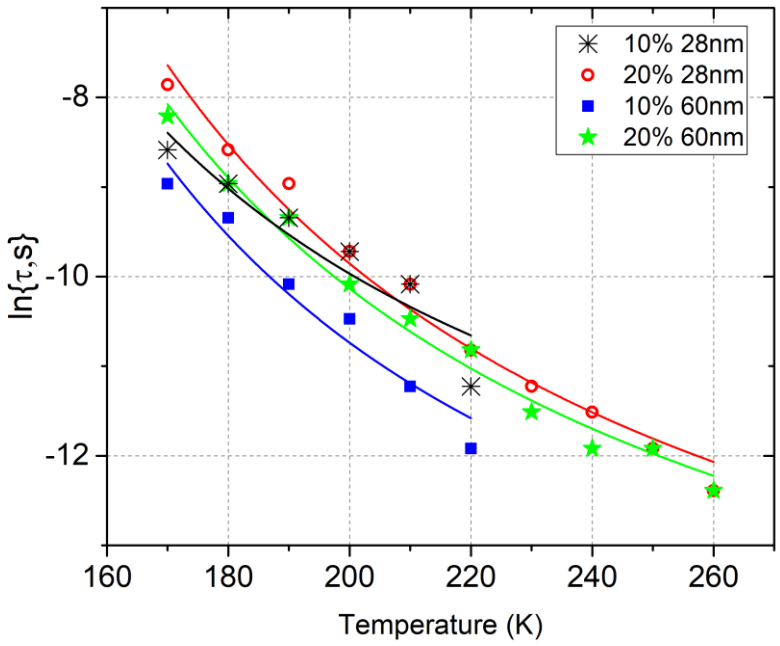

Figure 6. Temperature dependence of the relaxation time for $MnFe_2O_4$/epoxy composites below the percolation threshold. The solid lines are calculated according to Eq. (2).

In composites, the glass transition temperature decreases with the manganese ferrite concentration of any size compared to pure epoxy resin. Moreover, when concentration increase, the glass transition temperature slightly increases for smaller particles (28 nm) and decreases for larger particles (60 nm). For smaller particles, an increase with the concentration of the glass transition temperature is due to the decrease of the interfacial space between the polymer and nanoparticles, and the opposite situation is observed for larger particles.

3.3 Electrical conductivity

For composites below the percolation threshold (see, for example, Fig. 4, right) at high temperatures (above 380 K), the imaginary part of the dielectric permittivity increases strongly and becomes higher than the real part, which means that the composite has become conductive. Indeed (see Fig. 7) at high temperatures, the frequency dependence of the electrical conductivity demonstrates a frequency-independent plateau at low frequencies (corresponds to DC conductivity), and region increasing with frequency at high frequencies (corresponds to AC conductivity).

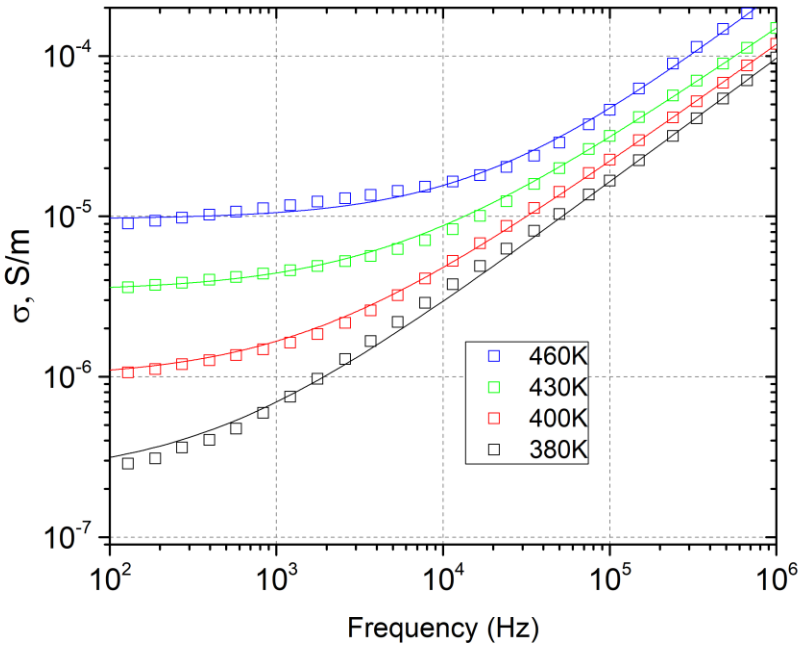

Figure 7. Frequency dependence of electrical conductivity for epoxy composite with 20 vol. % $MnFe_2O_4$ (60nm particle size) at different temperatures. The solid lines are calculated according to Eq. (3).

Therefore, the frequency dependence of the electrical conductivity can be fitted according to the universal power law:

$$\sigma = \sigma_{DC} + A\omega^s \quad (3)$$

where σ_{DC} is the DC conductivity and $A\omega^s$ is the AC conductivity. DC conductivity values for all investigated $MnFe_2O_4$/epoxy composites with 28 nm particle size are presented in Fig. 8.

For composites below the percolation threshold (10-25 vol. %) and for pure epoxy resin, DC conductivity values were obtained at higher temperatures only, above 380 K. This DC conductivity appearance is due to the epoxy resin becoming conductive at high temperature. σ_{DC} can be fitted by Arrhenius law: $\sigma_{DC} = \sigma_0 \exp\left(-\frac{E_A}{k_B T}\right)$, where σ_0 is the preexponential factor and E_A is the conductivity activation energy. Obtained parameters are present in Table 3. In composites, the conductivity activation energy decreases with filler concentration.

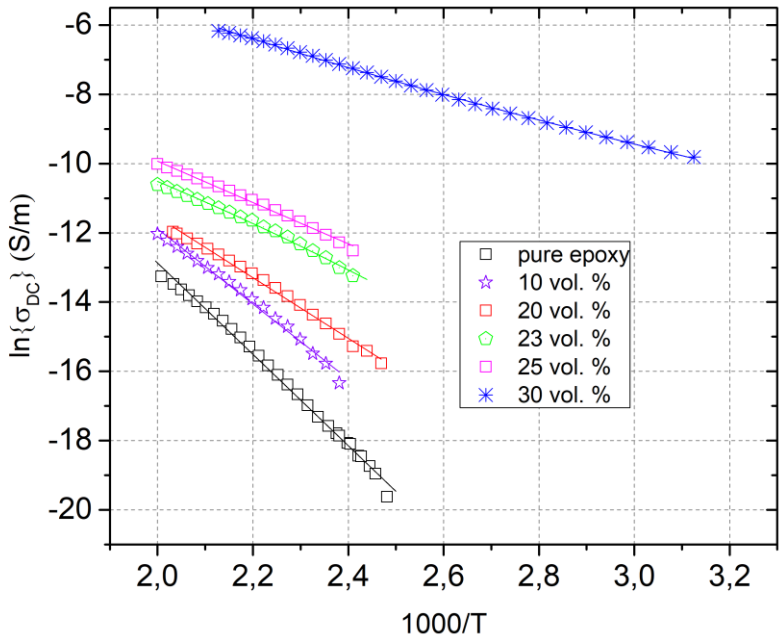

Figure 8. Temperature dependence of the DC electrical conductivity for $MnFe_2O_4$/epoxy composites with 28 nm particle size.

Table 3. Parameters of the Arrhenius law fit of the DC conductivity for $MnFe_2O_4$/epoxy composites with 28 nm particle size

	σ_0 (S/m)		E_A/k_B (K)	
	Value	Standard Error	Value	Standard Error
pure epoxy	$0.7 \cdot 10^6$	1.23	13185	90
10 vol. %	$0.2 \cdot 10^5$	1.79	10841	270
20 vol. %	$0.4 \cdot 10^3$	1.43	8745	160
23 vol.%	7.31	1.39	6247	153
25 vol. %	7.30	1.28	5961	114
30 vol. %	6.67	1.09	3791	33

For composites above the percolation threshold (30 vol. %), the DC conductivity is observed already at room temperature and also increases its absolute value during heating.
A similar conductivity behavior was observed for all other investigated $MnFe_2O_4$/epoxy composites with 60 nm particle size,.

4. Conclusion

Dielectric properties of epoxy composites containing the different additions of manganese ferrite ($MnFe_2O_4$) with two spherical particle size (28 and 60 nm) have been studied in the wide frequency range from 20 Hz to 1 MHz. It was demonstrated that the percolation thresholds in such systems are 30 and 29.3 vol.% for small and large $MnFe_2O_4$ particle, respectively. The small difference in the percolation threshold value is related with better distribution of larger nanoparticles. Above 380 K the electrical conductivity is typical for all composites, both below and above percolation threshold due to the electrical transport in polymer matrix. The activation energy strongly decreases with $MnFe_2O_4$ concentration

indicating that the electrical transport occurs together in $MnFe_2O_4$ and epoxy matrix subsystems.

Acknowledgenment
Lithuanian team acknowledge the support of Lithuanian Science Council according to the Lithuanian-Belorussian collaboration project (Nr. S-LB-19-8/(1.78)su-129). PK is supported by Horizon 2020 IF TURANDOT project 836816 and Academy of Finland Flagship Programme, Photonics Research and Innovation (PREIN), decision 320166.

References

[1] F. Qin, C. Brosseau, *J. Appl. Phys*. **2012**, *111* 6.
[2] Lubin G. Handbook of composites. – Springer Science & Business Media, 2013.
[3] M. Goodarz Naseri, E. Bin Saion, H. Abbastabar Ahangar, M. Hashim, A.H. Shaari, *Journal of Magnetism and Magnetic Materials* **2011**, *323* 1745.
[4] Z. X. Tang, C. M. Sorensen, K. J. Klabunde, G. C. Hadjipanayis, *Journal of Applied Physics* **1991**, *69*(8), 5279.
[5] J. Amighian, M. Mozaffari, B. Nasr, *Physica Status Solidi C* **2006**, *3(9)*, 3188.
[6] E. M. Mohammed, K. A. Malini, P. Kurian, M. R. Anantharaman, *Materials research bulletin* **2002**, *37(4)*, 753.
[7] B. Sahoo, S. K. Sahu, S. Nayak, D. Dhara, P. Pramanik, *Catalysis Science & Technology* **2012**, *2(7)*, 1367.
[8] P. Xiong, C. Hu, Y. Fan, W. Zhang, J. Zhu, X. Wang, *Journal of Power Sources* **2014**, *266*, 384.
[9] E. Peng, E. S. G. Choo, P. Chandrasekharan, C. T. Yang, J. Ding, K. H. Chuang, J. M. Xue, *Small* **2012**, *8(23)*, 3620.
[10] S. R. Ahmed, S. B. Ogale, G. C. Papaefthymiou, R. Ramesh, P. Kofinas, *Applied physics letters* **2002**, *80(9)*, 1616.
[11] R. Arulmurugan, G. Vaidyanathan, S. Sendhilnathan, B. Jeyadevan, *Journal of magnetism and magnetic materials* **2006**, *298(2)*, 83.
[12] J. B. Haun, T. J. Yoon, H. Lee, R. Weissleder, *Magnetic nanoparticle biosensors. Wiley Interdisciplinary Reviews: Nanomedicine and Nanobiotechnology* **2010**, *2(3)*, 291.
[13] K. J. Vinoy and R. M. Jha, Radar Absorbing Materials: From Theory to Design and Characterization, Kluwer Academic Publishers, Boston, 1996.
[14] P. Kuzhir, A. Paddubskaya, D. Bychanok, A. Nemilentsau, M. Shuba, A. Plusch, I. Sacco, *Thin Solid Films* **2011**, *519(12)*, 4114.
[15] D. Meisak, J. Macutkevic, J. Banys, D. Bychanok, P. Kuzhir, *International Journal of Nanoscience* **2019,** *18*, 1940018.
[16] A. Ameli, P. U. Jung, C. B. Park, *Carbon* **2013**, *60*, 379.
[17] E. Palaimiene, J. Macutkevic, J. Banys, A. Selskis, V. Fierro, A. Celzard, S. Schaefer, O. Shenderova, *Applied Physics Letters* **2018**, *113*, 033105.
[18] https://www.us-nano.com/inc/sdetail/7019
[19] https://www.us-nano.com/inc/sdetail/595
[20] D. Bychanok, P. Kuzhir, S. Maksimenko, S. Bellucci, and C. Brosseau, *Journal of Applied Physics* **2013**, *113*, 124103.
[21] D. van der Putten, J.T. Moonen, H.B. Brom, J.C.M. Brokken-Zijp, and M. A. J. Michels, *Physical Review Letters* **1992**, *69*, 494.
[22] Y. Sun, H.D. Bao, Z.X. Guo, and J. Yu, "Modeling of the electrical percolation of mixed carbon fillers in polymer-based composites," Macromolecules, vol. 42, pp. 459-463, 2009.
[23] A.K. Jonscher, *Nature* **1975**, *256*, 566.